INTERNATIONAL JOURNAL FOR NUMERICAL METHODS IN FLUIDS, VOL. 5, 995–1013 (1985)

A NUMERICAL STUDY OF THE APPLICABILITY OF THE BOUSSINESQ APPROXIMATION FOR A FLUID-SATURATED POROUS MEDIUM

D. K. GARTLING

Fluid Mechanics and Heat Transfer Division I, Sandia National Laboratories, Albuquerque, NM 87185, U.S.A

AND

C. E. HICKOX

Geothermal Research Division, Sandia National Laboratories, Albuquerque, NM 87185, U.S.A.

SUMMARY

The regions of applicability of the Boussinesq approximation are investigated for natural convection in a fluid-saturated porous medium. A perturbation method is used to assess the relative importance of individual terms in the differential equations which describe the natural convection process. Specific limits to the validity of the Boussinesq approximation are identified for water and air. For water, it is shown that the restrictions imposed by the classical Boussinesq approximation can be relaxed by allowing for the variation of thermophysical properties with temperature while still retaining the incompressible form of the continuity relation. Results of the analysis are verified through numerical calculations performed for steady natural convection in a planar, water-saturated porous region.

KEY WORDS Boussinesq Approximation Porous Media Finite Element

1. INTRODUCTION

The Boussinesq approximation[1] is a commonly employed assumption in both analytic and numerical studies of natural convection. Under the standard form of this simplifying assumption, the density of the fluid is treated as a constant everywhere except in the buoyancy term in the equations of motion. Also, the remaining fluid properties are assumed constant and viscous dissipation effects are neglected. This approximation was first suggested by Oberbeck,[2] prior to its use by Boussinesq, and is hereafter referred to as the Oberbeck–Boussinesq or OB approximation. When this approximation is invoked in the mathematical description of natural convection in a fluid-saturated porous medium, the resulting system of equations is composed of (1) an incompressible form of the continuity equation, (2) Darcy's law and (3) an energy transport equation. One of the prime motivations for using the OB approximation is that this simplified system of equations is significantly easier to analyse, either analytically or numerically, than the exact formulation.

The use of any approximation requires that the effects of the assumptions on the formulation and solution be well understood and quantified. In the present paper we have investigated three main aspects of the use of the OB approximation for flows in porous media. Using a method developed by Gray and Giorgini[3] we have first studied the limits of applicability of the standard or strict OB approximation. These results are in the form of allowable temperature differences

0271–2091/85/110995–19$01.90

Received 8 April 1985

and length scales for which a simplification of the complete equation system can be justified. The same analysis provides guidance in how the strict OB approximation can be relaxed such that the restrictions on the allowable temperature differences and length scale are increased without significantly increasing the complexity of the problem formulation. This relaxed or 'extended' OB approximation involves the retention of the restrictions on density variations while allowing the variation of all other material properties with pressure and temperature. In the third portion of the study we have used a numerical method to explore some of the consequences of using the strict and extended forms of the OB approximation for convective flows in an enclosure. In particular, we have examined the changes in the flow fields, temperature distributions and heat transfer rates to be expected when different formulations are employed.

Previous work in this area has concentrated on the effects of the OB approximation for ordinary natural convection described by the Navier–Stokes equations. MacGregor and Emery[4] explored the effects of a variable viscosity on convective flows in enclosures. Rubel and Landis[5] extended the previous work by considering variations in a number of material properties for flows at moderate Rayleigh number. Variable property boundary layer flows in water were analysed by Shaukatullah and Gebhart[6] and Leonardi and Reizes[7] presented a thorough study of variable property air flows in closed cavities. Several investigations[8,9] have examined the effect of variable fluid properties on the onset of convection in porous layers. Also, Ribando and Torrance[10] presented solutions that illustrate the effects of a variable viscosity and permeability on finite amplitude convection in rectangular enclosures. Despite the interest in using various forms of the OB approximation, relatively little attention has been focused on the problem of defining the limits of applicability of these formulations for porous flow problems. It is this topic that is addressed here.

2. MATHEMATICAL SYSTEMS STUDIED

2.1. *Complete system*

In this section we identify a mathematical representation which is appropriate for the description of natural convection in a homogeneous, isotropic, porous medium and which forms the basis for subsequent analytical and numerical investigations. The porous matrix is assumed to be rigid and in thermal equilibrium with the saturating fluid. It is further assumed that the fluid motion can be adequately described by Darcy's law. Equations expressing conservation of mass, Darcy's law, and thermal energy transport have the forms

$$\phi \frac{\partial \rho}{\partial t} + \operatorname{div}(\rho \mathbf{v}) = 0, \tag{1}$$

$$\frac{\mu}{k}\mathbf{v} = -\operatorname{grad} P - \rho g \operatorname{grad} h, \tag{2}$$

$$(\rho C_p)_e \frac{\partial T}{\partial t} + \rho C_p \mathbf{v} \cdot \operatorname{grad} T = \operatorname{div}(K_e \operatorname{grad} T), \tag{3}$$

where $\mathbf{v}$ is the bulk volume-averaged Darcy velocity, P is the pore volume averaged pressure, and T is the temperature. In equation (3) we have neglected the effects of pressure variations as well as viscous dissipation of energy. The symbols $\phi, \rho, C_p, \mu, k, g$ and K denote, respectively, porosity, density, specific heat, viscosity, permeability, acceleration due to gravity and thermal conductivity. The elevation h is measured vertically upward. The subscript e denotes effective

properties which are related to the fluid and solid matrix properties by the assumed relations

$$(\rho C_p)_e = \phi \rho C_p + (1-\phi)(\rho C_p)_s, \tag{4}$$

$$K_e = \phi K + (1-\phi) K_s, \tag{5}$$

where the subscript s identifies solid matrix properties and properties without a subscript are those of the fluid. In general, the fluid properties ρ, C_p, μ and K depend on temperature and pressure. Solid matrix properties as well as porosity and permeability are assumed constant.

The mathematical system described by equations (1)–(5), together with appropriately specified thermophysical properties and boundary conditions, constitutes what we shall refer to as the 'complete', or exact, system for the description of transient natural convection in a homogeneous, isotropic, fluid-saturated porous medium. The primary additional restriction which must be placed on the validity of this system is that the velocity must be low enough to ensure the applicability of Darcy's law. Darcy's law is generally valid so long as the Reynolds number based on the square root of the permeability and the Darcy velocity is less than unity.[11] For such low velocities, the neglect of pressure work and viscous dissipation can generally be justified.

2.2. *Oberbeck–Boussinesq (OB) systems*

The OB approximation requires that the fluid density be treated as constant everywhere except in the body force term in the equation of motion. For purposes of the present paper, we define a 'strict' OB system as the system of equations which results when the OB approximation is invoked with regard to the density variation and it is further assumed that all remaining thermophysical properties are constant. Under the stated assumptions, equations (1)–(3) become

$$\operatorname{div}(\mathbf{v}) = 0, \tag{6}$$

$$\frac{\mu}{k}\mathbf{v} = -\operatorname{grad} P - \rho g \operatorname{grad} h, \tag{7}$$

$$(\rho_0 C_p)_e \frac{\partial T}{\partial t} + \rho_0 C_p \mathbf{v} \cdot \operatorname{grad} T = K_e \operatorname{div}(\operatorname{grad} T), \tag{8}$$

where the zero subscript indicates a constant reference fluid density and effective properties are obtained from equations (4) and (5). Equations (6)–(8) will be referred to as the strict OB system in subsequent discussions.

If we retain the OB approximation, but relax the additional restriction requiring that all thermophysical properties, other than fluid density, remain constant, we obtain a system of equations which we shall refer to as the 'extended' OB system, following the convention adopted by Gray and Giorgini.[3] This system of equations can be obtained from equations (6)–(8) by replacing the right-hand-side of equation (8) with div (K_e grad T), to account for the variability of the thermal conductivity.

3. ANALYSIS OF THE OBERBECK–BOUSSINESQ APPROXIMATION

In this section, we shall deduce the conditions for which we are justified in replacing the complete system, given by equations (1)–(3), with the strict OB system as given by equations (6)–(8). Furthermore, we shall investigate the advantages attained through implementation of the extended OB system.

3.1. Non-dimensional equations

In order to recover the strict OB system from equations (1)–(3), a number of terms must be eliminated. The justification for neglecting the various terms is obtained by application of the perturbation approach used by Gray and Giorgini in their study of the OB approximation for ordinary natural convection involving liquids and gases.

It is first assumed that the fluid properties can be represented by the linearized Taylor series expansions:

$$\rho = \rho_0[1 - \beta_0(T - T_0) + \gamma_0(P - P_0)], \tag{9a}$$

$$C_p = C_{p0}[1 + a_0(T - T_0) + b_0(P - P_0)], \tag{9b}$$

$$\mu = \mu_0[1 + c_0(T - T_0) + d_0(P - P_0)], \tag{9c}$$

$$K = K_0[1 + e_0(T - T_0) + f_0(P - P_0)], \tag{9d}$$

where the subscript 0 represents the reference state (T_0, P_0) and all coefficients are constant. Although the use of linearized Taylor series expansions can generally be justified, care must be exercised when considering fluids, such as water, which exhibit a density maximum.

Next, the differential equations are rendered non-dimensional, through the choice of suitable scales, so that all functions of the non-dimensional variables are, at most, of order unity. This is accomplished through the introduction of a characteristic length scale L, a characteristic temperature difference θ, and a buoyancy velocity scale $\rho_0 g\beta_0\theta k/\mu_0$. The corresponding reference time is then given by $\mu_0 L/\rho_0 g\beta_0\theta k$. Dynamic pressures, i.e. the difference between local pressure and the pressure in the static state, are scaled by $(\rho_0 g\beta_0\theta L)$. Pressure differences between local conditions and the reference state, as well as derivatives of pressure, are scaled by $(\rho_0 gL)$.

Application of the scaling factors to equations (1)–(5) produces a non-dimensional system of equations. This latter system includes the Rayleigh number, $\rho_0^2 C_{p0} g\beta_0\theta kL/K_{e_0}\mu_0$, as a parameter. In addition, there result eight parameters which are denoted by ε_1 to ε_8. For details of the non-dimensionalization, as applied to ordinary natural convection, Reference 3 should be consulted. The current application closely parallels that of Reference 3 except that a generalization of Darcy's law is used instead of the Navier–Stokes equations and the continuity and thermal energy transport equations are modified for application to porous media.

A brief illustration of the technique is afforded by consideration of the continuity relation, equation (1). Application of the appropriate scaling parameters, together with equation (9a), provides the following result

$$-\varepsilon_1\left(\phi\frac{\partial\hat{T}}{\partial\tau} + \hat{\mathbf{v}}\cdot\operatorname{grad}\hat{T}\right) + \varepsilon_2\left(\phi\frac{\partial\hat{P}}{\partial\tau} + \hat{\mathbf{v}}\cdot\operatorname{grad}\hat{P}\right) + [1 - \varepsilon_1(\hat{T} - \hat{T}_0) + \varepsilon_2(\hat{P} - \hat{P}_0)]\operatorname{div}\hat{\mathbf{v}} = 0, \tag{10}$$

where τ is the non-dimensional time, the circumflex indicates a non-dimensional quantity, $\varepsilon_1 = \beta_0\theta$ and $\varepsilon_2 = \gamma_0\rho_0 gL$. Anticipating a later result, we note that in order to recover the incompressible form of the continuity relation it is necessary that the absolute values of ε_1 and ε_2 be small when compared with unity; thus indicating restrictions on the allowable temperature difference and length scale.

Darcy's law and the energy transport relation are rendered non-dimensional by the straightforward, but somewhat lengthy, application of the scaling factors which have been described. The ε-parameters which result are defined in Table I along with an indication of the equations in which they appear.

Table I: Definitions of ε-parameters

Parameter	Definition	Applicable equation
ε_1	$\beta_0\theta$	1,3
ε_2	$\gamma_0\rho_0 gL$	1,2,3
ε_3	$c_0\theta$	2
ε_4	$d_0\rho_0 gL$	2
ε_5	$a_0\theta$	3
ε_6	$b_0\rho_0 gL$	3
ε_7	$e_0\theta$	3
ε_8	$f_0\rho_0 gL$	3

Table II. Properties of water and air at 15 °C and 1 atm, from Reference 3

Property	Water	Air	Units
ρ_0	1·0	$1{\cdot}2 \times 10^{-3}$	gm/cm^3
C_{ρ_0}	4·2	1·0	J/gm °C
μ_0	$1{\cdot}0 \times 10^{-2}$	$1{\cdot}7 \times 10^{-4}$	gm/cm s
K_0	$5{\cdot}9 \times 10^{-3}$	$2{\cdot}5 \times 10^{-4}$	J/cm s° C
β_0	$1{\cdot}5 \times 10^{-4}$	$3{\cdot}5 \times 10^{-3}$	1/°C
γ_0	$4{\cdot}9 \times 10^{-11}$	$1{\cdot}0 \times 10^{-6}$	cm^2/dyne
a_0	$-2{\cdot}4 \times 10^{-4}$	$4{\cdot}5 \times 10^{-5}$	1/°C
b_0	$-2{\cdot}5 \times 10^{-10}$	$1{\cdot}9 \times 10^{-9}$	cm^2/dyne
c_0	$-2{\cdot}7 \times 10^{-2}$	$2{\cdot}8 \times 10^{-3}$	1/°C
d_0	$-2{\cdot}7 \times 10^{-11}$	0	cm^2/dyne
e_0	$1{\cdot}7 \times 10^{-3}$	$2{\cdot}4 \times 10^{-3}$	1/°C
f_0	$4{\cdot}3 \times 10^{-10}$	0	cm^2/dyne

Evaluation of the ε's requires a knowledge of certain specific fluid properties. Values for these properties, adapted from Reference 3, are summarized in Table II for water and air at 15 °C and 1 atm, and will be used to illustrate the application of the derived results.

3.2. *Application of the results*

Upon consideration of the non-dimensional results, it can be shown that, in order to recover the strict OB system, equations (6)–(8), from the complete system, equations (1)–(3), it is necessary that the absolute value of each $\varepsilon_n (n = 1, 2, 3, \ldots, 8)$ be small when compared with unity. For water, the most restrictive of these requirements for the allowable temperature difference and length scale are, respectively, $\varepsilon_3 \ll 1$ and $\varepsilon_8 \ll 1$. For air, the corresponding requirements are $\varepsilon_1 \ll 1$, and $\varepsilon_2 \ll 1$. Upon assuming a value of 0·1 for the ε's, the information in Tables I and II can be used to produce numerical estimates of the allowable temperature differences and length scales for water and air. The results are summarized in the first two columns of Table III. At this point, the most significant observation that can be made from Table III is that the strict OB system is limited in application to a characteristic temperature difference of only 3·7 °C for water and 28·6 °C for air. This result is similar to the restrictions applicable to the use of the strict OB system for ordinary natural convection.

Investigation of the limits of applicability for the extended OB system results in the new requirements that $\varepsilon_1 \ll 1$ and $\varepsilon_2 \ll 1$ for water. The requirements for air are unchanged from

Table III. Allowable temperature and length scales predicted for Boussinesq systems

Fluid	Strict Boussinesq θ(°C)	Strict Boussinesq $L(m)$	Extended Boussinesq θ(°C)	Extended Boussinesq $L(m)$
Water	3·7	2373	667*	20,825
Air	28·6	850	28·6	850

* Violates linear assumption, actually $\theta \sim 100\,°C$

those necessary for the strict OB system. If a value of 0·1 is again assumed for the ε's, then the results tabulated in the last two columns of Table III are obtained. For water, it is immediately obvious that the range of applicability of the extended Boussinesq system is significantly wider than that associated with the strict OB system. The predicted allowable temperature difference of 667 °C obviously violates the assumption of linearity used in the analysis. The true physical requirement is simply that the maximum density change which results from a characteristic temperature difference must be small when compared with the reference density ρ_0. Taking into account the non-linearity of the density–temperature relation for water and using the reference conditions of Table II, we conclude that the allowable temperature difference is $O(100\,°C)$ for the extended OB system. The increased range of validity associated with the extended OB system, for water, is primarily a result of the relatively strong temperature dependence of the viscosity. Hence, by simply allowing for the variation of physical properties with temperature, we are able to significantly extend the region of validity of the OB approximation for liquids such as water. Except for extremely large-scale motions, the restrictions imposed by pressure differences are not anticipated to exert a controlling influence on the applicability of the equations. For laboratory-scale experiments, or applications to typical insulation systems, we need be concerned only with the restrictions imposed by temperature differences.

We should note that the actual numerical values presented for the allowable temperature differences and length scales (Table III) are somewhat arbitrary since they depend directly on assumed values for the ε's in the perturbation analysis. The choice of $\varepsilon = 0{\cdot}1$ is reasonable for enforcing the condition that $\varepsilon \ll 1$. Such a choice implies that, at most, the error in satisfying the conservation of mass equation will be 10 per cent. Unfortunately, there is no way to relate this error magnitude to changes or errors in the field variables (i.e. $\mathbf{v}, P, T$) and thus know quantitatively how well an OB system will approximate the complete equation set. The numerical studies to be described in a subsequent section will be used to resolve this dilemma.

4. NUMERICAL STUDIES

The results of the perturbation analysis have shown that by employing the extended OB approximation in lieu of the strict OB formulation, larger temperature differences and length scales may be used in porous flow problems without significant deviation from an incompressible continuity equation. Unfortunately, the analysis is not able to provide precise, verifiable bounds on the allowable temperature differences; this information must come from a direct comparison of solutions for the various formulations. In this section we present a numerical study of natural convection in a simple porous region with a view toward quantifying the differences in the previously described formulations. The previous results indicate that the advantages of the extended Boussinesq system are realized only when the saturating fluid viscosity exhibits a

relatively strong temperature dependence. For this reason, we will be concerned with a porous region that is saturated with water. Furthermore, it has also been shown that property variations with pressure are unimportant in laboratory-scale experiments. Also, a consideration of the information in Tables I and II shows that, for water, the variation of specific heat with temperature and pressure is significantly less important than the variations of the other physical properties. We have thus elected to treat the specific heat as constant and to include only the effects of temperature variations on the other fluid properties (ρ, μ, K) in the numerical simulations.

4.1. Problem geometry

The geometry used in the numerical simulations is illustrated in Figure 1. A fluid-saturated, planar, porous bed is contained within a square enclosure which measures 1 m on a side. All boundaries are impermeable. The upper and lower boundaries are perfectly insulated and a constant temperature difference is imposed between the vertical side walls, with each side wall maintained at a uniform temperature. The higher temperature wall is on the right. The temperatures of the side walls are raised or lowered by equal amounts relative to the mean reference temperature of the enclosure which is held constant at 47 °C for all calculations. It is assumed that the porous region is nominally at a mean pressure of 1 atm, hence maximum and minimum side wall temperatures are restricted to 90 °C and 4 °C, respectively.

It is assumed that the porous matrix is composed of glass (S_iO_2) spheres. Depending on the geometry of the packing, the porosity of a bed of spheres can vary between 0·260 and 0·476. In all calculations, the sphere diameter d, porosity ϕ and permeability k were chosen to be commensurate with the Kozeny–Carman equation[12]

$$k = d^2\phi^3/180(1-\phi)^2. \tag{11}$$

Specifically, a diameter of 0·1 cm and a porosity of 0·26 were selected for the numerical simulations. All physical properties of the glass were assumed constant. Values of the physical properties and expressions for the temperature dependence of the fluid properties are summarized in the Appendix. The geometry, materials and boundary conditions were selected to be representative of a laboratory experiment.

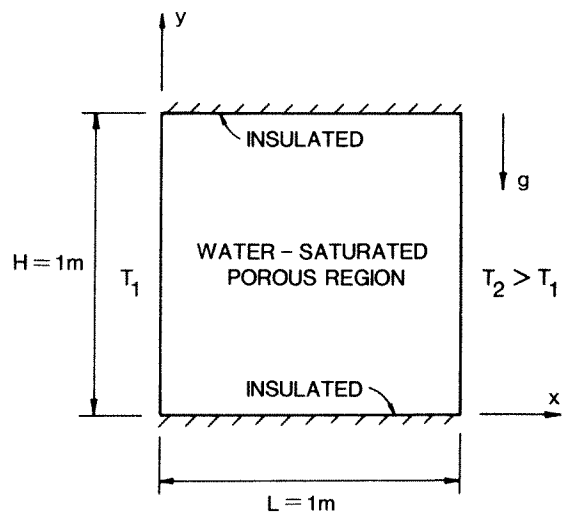

Figure 1. Schematic diagram of the geometry used for the numerical simulations

4.2. Computational approach

Numerical solutions for the example problem described in the previous section were obtained with a finite element computer program. Since a complete description of this program is available elsewhere[13,14] we shall not discuss the details of the numerical method in the present paper. The computer program is based on the Galerkin form of the finite element method and is primarily designed to provide numerical solutions to both the strict and extended OB systems. The program has been extensively tested, compared to analytic and numerical solutions[15,16] and benchmarked against experimental data.[17,18]

In order to carry out the study of interest, numerical solutions to the fully compressible equations were also required. These solutions were obtained from the same basic finite element program, a situation that was made possible by a judicious change of variables. Limiting attention to the steady flow case, we define a new velocity variable as $\mathbf{v}' = \rho\mathbf{v}/\rho_0$, where $\mathbf{v}$ is the usual Darcy velocity. Substituting this new variable into the complete system of equations (1)–(3) produces the following system:

$$\operatorname{div}\mathbf{v}' = 0, \tag{12}$$

$$\frac{\rho_0\mu}{\rho k}\mathbf{v}' = -\operatorname{grad}P - \rho g \operatorname{grad}h, \tag{13}$$

$$\rho_0 C_p \mathbf{v}' \cdot \operatorname{grad}T = \operatorname{div}(K_e \operatorname{grad}T). \tag{14}$$

Mathematically, these equations are identical to the extended OB system, for steady flow, where the fluid viscosity is replaced by $\rho_0\mu/\rho$. Hence, numerical solutions to the complete system can be obtained from a numerical model which uses the OB approximation, but allows for the variation of thermophysical properties other than fluid density, i.e. the extended OB approximation. We were thus able to solve all three equation systems of interest with the same numerical method by simply re-interpreting variables and allowing the appropriate variation of material properties.

For purposes of analysis, the porous region was discretized using a 20×20 mesh of eight-node quadrilateral elements. Most solutions were obtained using a uniform element spacing. However, in order to assess the adequacy of the uniform grid, gradations in element size ranging up to a ratio of 16:1 were used for selected cases, to provide increased resolution near boundaries, and the results compared with those obtained using the uniform grid. It was found that the uniform grid provided acceptable results, and was therefore used for most of the calculations. Based on studies which we have reported previously[15,16] it is concluded that the number of elements used in the analysis is significantly larger than that required for acceptable accuracy.

5. RESULTS OF THE NUMERICAL STUDIES

In this section we describe the results of the numerical studies for the three systems of equations under consideration.

5.1. Heat transfer rates

The effect of the two OB approximations on the overall heat transfer rate across the enclosure is illustrated in Figure 2. Heat transfer rates predicted from the strict and extended OB systems are compared with those computed using the complete system of equations as a plot of the

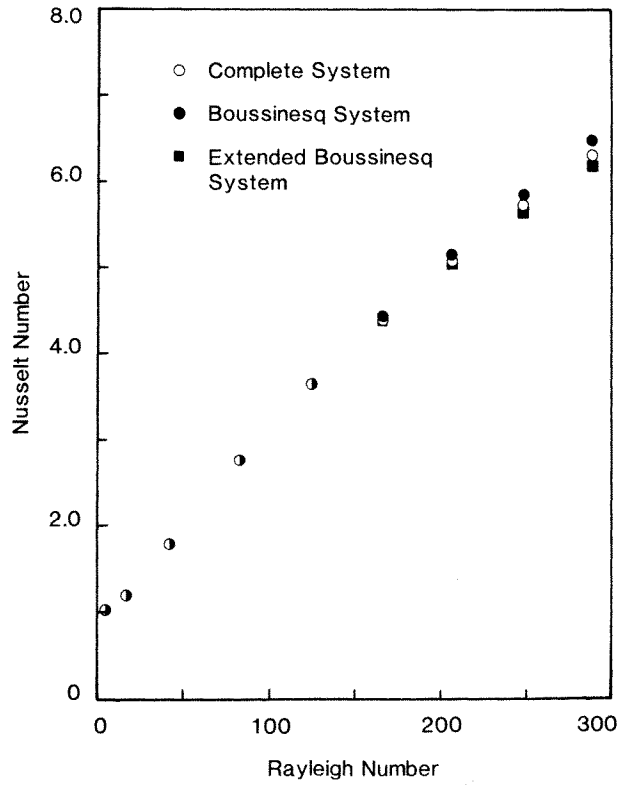

Figure 2. Nusselt number against Rayleigh number for the enclosure geometry and three equation systems

Nusselt number

$$Nu = QL/K_e\Delta TH = Q/K_e\Delta T \tag{15}$$

against the Rayleigh number

$$Ra = \rho_0^2 C_{p0} g\beta_0 kL\Delta T/\mu_0 K_{e0}. \tag{16}$$

In equations (15) and (16) all properties were evaluated at the mean temperature of the cavity (47 °C), Q is the total heat transfer rate across the enclosure, and ΔT is the imposed temperature difference across the enclosure. The results of Figure 2 represent overall temperature differences ranging from 1 °C to 70 °C. The total heat transfer rate across the enclosure (Q) was evaluated by computing the local heat flux in those finite elements adjacent to the vertical boundaries and then employing a simple quadrature rule to integrate the resulting flux distribution. Overall heat transfer rates computed on the two boundaries agreed within a tolerance of ± 1 per cent for all Rayleigh numbers.

It is obvious from the computed results that the use of either OB system does not strongly influence the overall heat transfer rate. At the higher Rayleigh numbers the strict OB overpredicts the Nusselt number whereas the extended OB result is below the results for the complete system. The maximum difference in Nusselt number for all three equation systems is less than 5 per cent at the highest Rayleigh number considered in this study.

The limited extent to which the Nusselt number is influenced by property variations can be deduced, mathematically, from a consideration of the symmetry properties exhibited by the

system of equations. For water, the most pronounced property variation is associated with the temperature dependence of the viscosity. Hence, it is sufficient to consider only this effect in assessing the influence of property variations on the Nusselt number. Consider the steady-state form of the extended OB equations (6)–(8) and represent the viscosity by equation (9c), neglecting the effect of pressure changes ($d_0 = 0$). Following the general approach outlined by Rubel and Landis[5] the pressure is eliminated by cross-differentiation of Darcy's law and a stream function ψ is introduced to satisfy the continuity equation. Since it is convenient to use the non-dimensional form of the resulting equations, we adopt the scaling parameters introduced in section 3.1 and note that the stream function is made non-dimensional through division by the reference velocity and length scale. The stream function and temperature are then expanded in regular perturbation series in terms of the small parameter $\varepsilon = c_0\theta$. At zeroth order, the strict OB equations are recovered and, to first-order, equations are obtained that express the first-order effects of viscosity variation. Symmetry properties associated with these perturbation equations can then be used to deduce the extent to which the viscosity variation affects the overall heat transfer rate across the enclosure.

Mathematically, the structure of the strict OB equation dictates that the solution to this system possess a certain symmetry. Specifically, for the geometry and co-ordinates of Figure 1, if $\hat{\Psi}(\xi,\eta)$, $\hat{T}(\xi,\eta)$ denote non-dimensional solutions to the strict OB system, where $\hat{T}$ is defined by $(T - T_0)/\theta$ and $(\xi,\eta) = (x,y)/L$, then it can be demonstrated by direct substitution[19,20] that the equations are invariant under the transformation $\hat{\Psi}(\xi,\eta) = \hat{\Psi}(\bar{\xi},\bar{\eta})$, $\hat{T}(\xi,\eta) = -\hat{T}(\bar{\xi},\bar{\eta})$ where $\bar{\xi} = 1 - \xi$ and $\bar{\eta} = 1 - \eta$. Hence, $\hat{\Psi}(\bar{\xi},\bar{\eta})$ and $-\hat{T}(\bar{\xi},\bar{\eta})$ are also solutions. This resulting 'centro'-symmetry places a strong constraint on solutions to the strict OB system that is not present in either of the other two systems studied. Solutions to the first-order perturbation equations exhibit the following symmetry: $\hat{\Psi}_1(\xi,\eta) = -\hat{\Psi}_1(\bar{\xi},\bar{\eta})$ and $\hat{T}_1(\xi,\eta) = \hat{T}_1(\bar{\xi},\bar{\eta})$.

Using the symmetry properties described above plus the requirement that the average Nusselt numbers evaluated on either vertical boundary be identical, allows the average Nusselt number for the enclosure to be determined as

$$Nu = Nu_0 + O(\varepsilon^2), \tag{17}$$

where Nu_0 is the Nusselt number associated with the strict OB system of equations and the $O(\varepsilon^2)$ term represents the correction due to viscosity variation. There is no first-order correction to the heat transfer rate. For the parameters used in the numerical study, the maximum value of ε is 0·95. Thus, the maximum correction to the Nusselt number is of the order of 0·89. A consideration of Figure 2 shows that the actual computed effect is approximately one-third of the estimated value. However, the estimate is certainly valid to an order-of-magnitude. We thus conclude that the lack of sensitivity of the heat transfer rate to the equation system selected is supported by theoretical considerations.

5.2. *Thermal and flow fields*

Although the heat transfer rate is not strongly influenced, the predicted flow field can be significantly affected by the particular choice of the system of equations chosen for its description. As an example, in Figure 3 we show plots of the computed isotherms and streamlines associated with each of the three mathematical systems studied for a Rayleigh number of 207·5, corresponding to an overall temperature difference of 50 °C. This particular set of comparative calculations was performed on a non-uniform mesh in order to better resolve the important features of the flow field. A horizontal mesh gradation was used with element widths on the vertical boundaries being a factor of eight smaller than those on the midplane of the enclosure. A temperature

difference of 50 °C was chosen since it represents an approximate order of magnitude increase over the maximum allowable temperature difference predicted for the strict OB system. In the Figure, isotherms are equally spaced between a value of 72 °C on the hot wall and 22 °C on the cooler wall. Streamlines are equally spaced between a value of zero on the boundary and the maximum value of the stream function quoted for each plot. The location of the maximum stream function is indicated by a small cross.

Upon comparing the plots in Figure 3, it is observed, as anticipated from the heat transfer results, that the thermal fields exhibit relatively little sensitivity to the system of equations chosen for the description of the natural convection process. The streamline distribution is, however, noticeably affected. A strong asymmetry results from the use of the complete system which is due, primarily, to the relatively strong variation of the viscosity of water with temperature. The good agreement obtained between the results of the complete system and those of the extended OB system further supports this observation.

The solutions to the complete and extended OB system show a progressive deviation from the centro-symmetric solution of the strict OB system (as described in section 5·1) with increasing Rayleigh number (i.e. increasing ΔT). This trend is illustrated in Figure 4 where vertical velocity

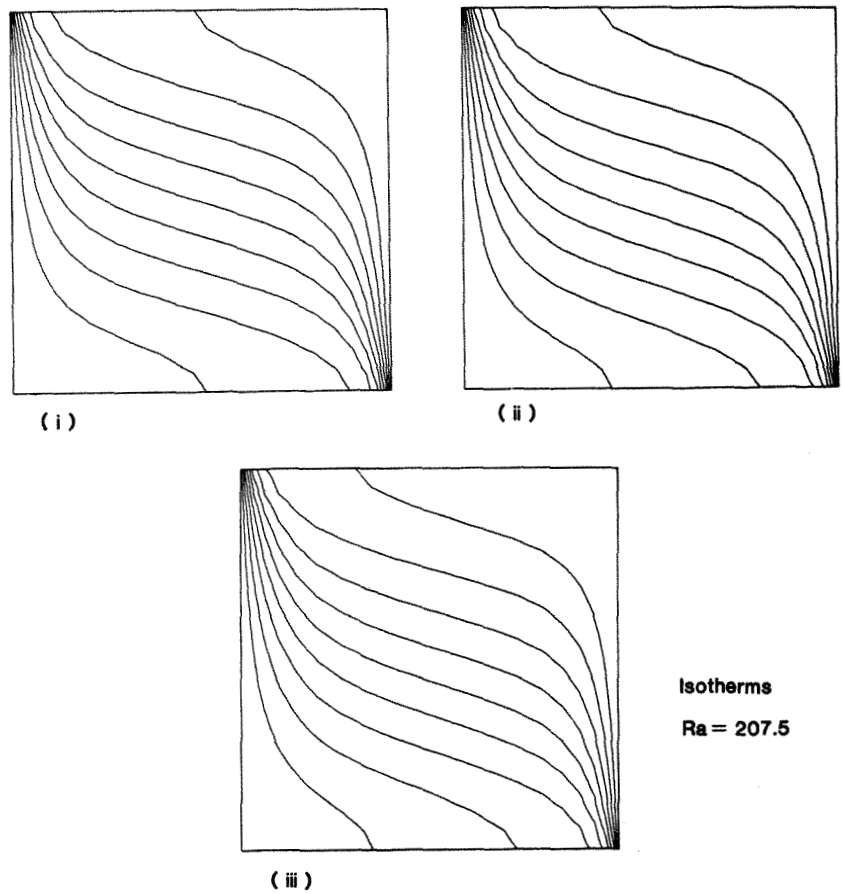

Figure 3(a). Isotherms calculated for the enclosure geometry for each of the equation systems studied: (i) strict OB; (ii) extended OB; (iii) complete. $Ra = 207{\cdot}5$, $\Delta T = 50\,°C$

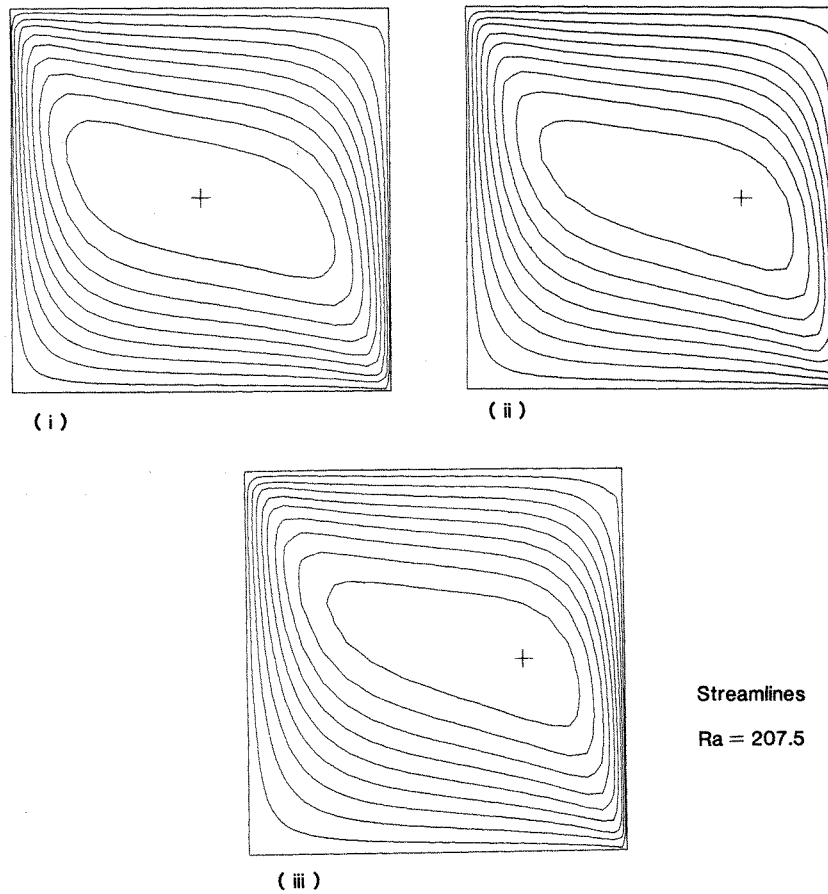

Figure 3(b). Streamlines calculated for the enclosure geometry for each of the equation systems studied: (i) strict OB, $\Psi_{max} = 0{\cdot}234 \times 10^{-5}\,m^2/s$; (ii) extended OB, $\Psi_{max} = 0{\cdot}257 \times 10^{-5}\,m^2/s$; (iii) complete, $\Psi_{max} = 0{\cdot}245 \times 10^{-5}\,m^2/s$. $Ra = 207{\cdot}5$, $\Delta T = 50\,^{\circ}C$

profiles taken across the cavity mid-height are shown for three different Rayleigh numbers. Note that the plotted velocity field has been made non-dimensional with a reference (buoyancy) velocity defined by $v_{ref} = \rho g \beta \Delta T k/\mu$. At the lower Rayleigh number all three systems produce very similar, symmetric profiles (Figure 4(a)). For intermediate Rayleigh numbers the extended OB and complete system solutions begin to develop an asymmetry in the velocity profile with the higher velocities occurring on the hot wall. The highest Rayleigh number cases show very strong asymmetries and noticeable differences between the solutions for all three equations systems. Note that pointwise, differences between the strict OB and complete system solutions are as large as 100 per cent near the cold wall.

For the purpose of later discussion we have attempted to quantify the differences between the numerical solutions for the various equation systems considered. Shown in Figures 5 and 6 are plots of the norm of the difference between two solution quantities against the Rayleigh number and imposed temperature difference. In each case the discrete l_2 norm was used which is defined by

$$N_x = \|\mathbf{x} - \mathbf{x}^{cs}\| = \frac{1}{n}\left[\sum_{i=1}^{n} (x_i - x_i^{cs})^2\right]^{1/2} \tag{18}$$

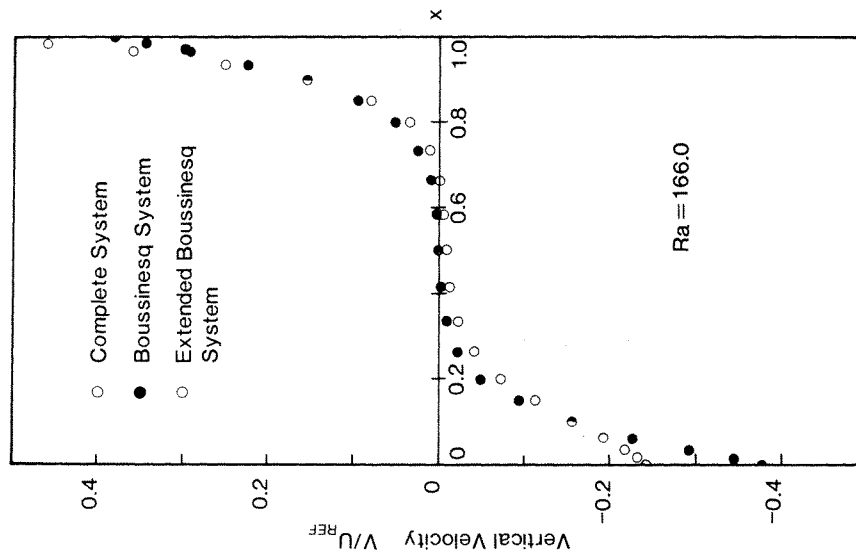

Figure 4(b). Vertical velocity profile along the horizontal mid-plane of the enclosure, $Ra = 166{\cdot}0$

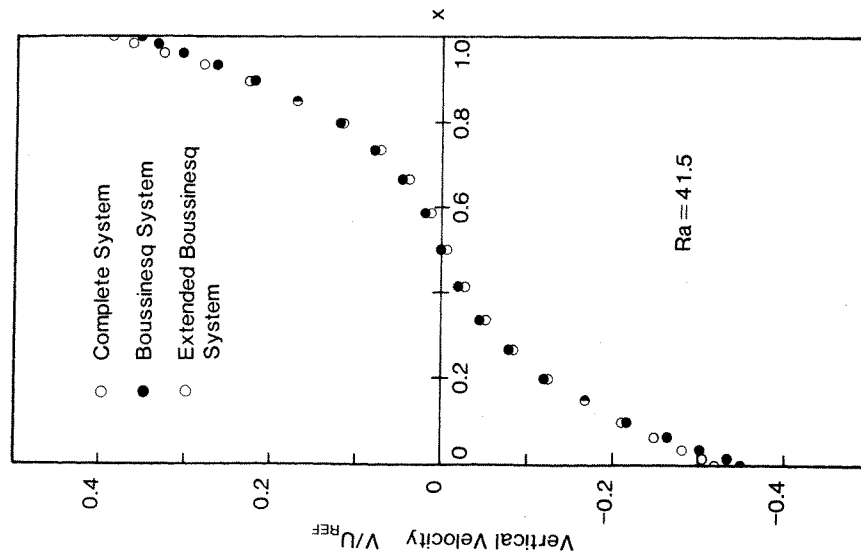

Figure 4(a). Vertical velocity profile along the horizontal mid-plane of the enclosure, $Ra = 41{\cdot}5$

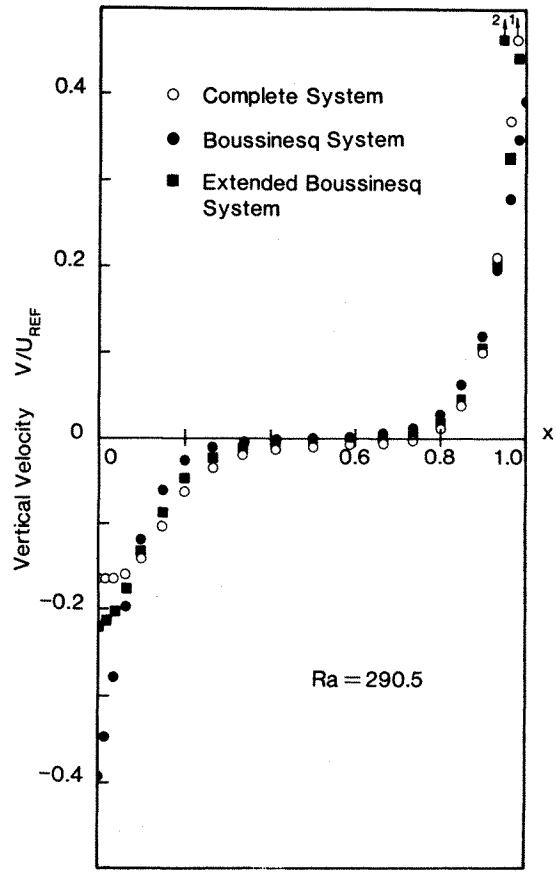

Figure 4(c). Vertical velocity profile along the horizontal mid-plane of the enclosure, $Ra = 290{\cdot}5$. Note: Points 1 and 2 have ordinate values of 0·66 and 0·52, respectively

where n is the number of solution points considered, x_i is a solution variable for either the strict or extended OB system and x_i^{cs} is a solution variable for the complete equation system. Each norm is thus taken with respect to the solution for the complete equation system. The solution variables used for comparison were the normalized values of the velocity and local heat flux; the velocity was normalized by the buoyancy velocity defined previously, and the local heat flux was normalized by a conductive heat flux defined by $q_{ref} = K_e \Delta T/L$. To simplify the computations the norm was taken over the n points in a one-dimensional profile within the cavity. The velocity profile was located at the mid-height of the cavity (same profile as shown in Figure 4) and the flux profile was located along the vertical (hot) wall. These locations were selected as showing representative (large) differences between the various solutions.

It is apparent from Figures 5 and 6 that the extended OB approximation always produces a solution that is 'closer' to the complete equation solution than the strict OB approximation. This result is, in effect, a restatement of the result produced by the perturbation analysis. For a specified accuracy (i.e. difference relative to the complete equation solution) the extended OB approximation can be used over a wider range of temperature differences than the strict OB approximation. Based on the limited data in Figures 5 and 6 the increase in allowable temperature difference for the extended OB approximation is a factor of $\sim (1{\cdot}5\text{–}2{\cdot}5)$ larger than for the strict OB approximation.

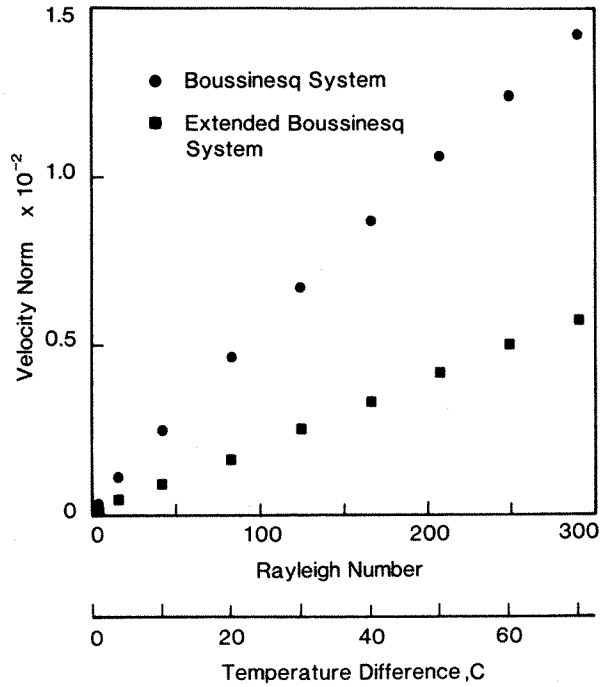

Figure 5. Variation of the norm of velocity differences with Rayleigh number and imposed temperature difference

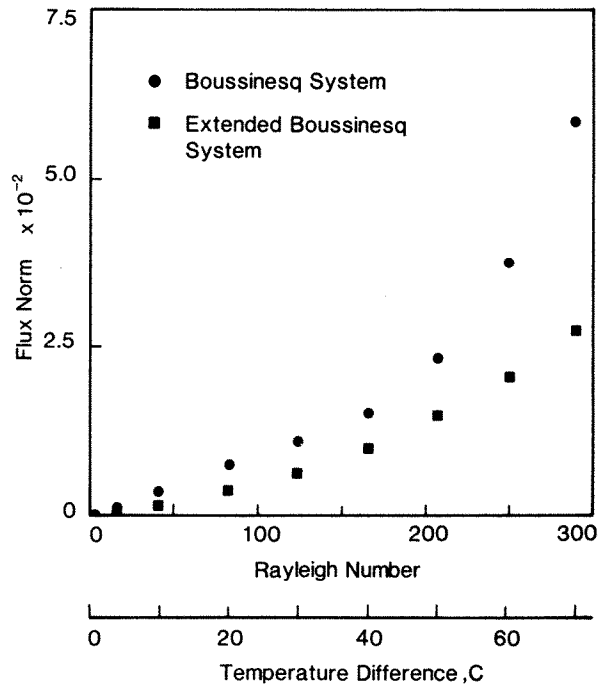

Figure 6. Variation of the norm of heat flux differences with Rayleigh number and imposed temperature difference

The smaller (1·5) factor is controlled by the accuracy of the heat flux, whereas the larger (2·5) factor is dictated by the velocity norms. These factors must only be regarded as rough approximations since the variation of the norms with Rayleigh number (and ΔT) is not linear. However, we note that the (1·5–2·5) increase in allowable temperature difference predicted from the numerical solutions is roughly an order of magnitude less than the increase predicted by the perturbation analysis (see Table III).

6. DISCUSSION AND CONCLUSIONS

At the outset of this study our primary objective was to answer the following two questions: (i) Over what range of temperature differences does the strict OB approximation produce a valid description of natural convection in a porous medium? and (ii) Can the extended OB approximation be used to advantage in this class of problems? We employed two different, but complementary, techniques to try to answer these questions and provide 'rules-of-thumb' for using the OB approximation. Our success in reaching these objectives is assessed in the present section.

The perturbation analysis of section 3 provided a systematic method for evaluating various forms of the OB approximation and, in fact, permitted a quantitative estimate for the acceptable range of temperature differences for each system of equations. Unfortunately, the quantitative results of this analysis are predicted on an assumed tolerance for the satisfaction of the incompressibility constraint. This tolerance cannot be related to accuracy estimates on the primary dependent variables (e.g. velocity, temperature) and therefore, no obvious judgement can be made on the temperature difference estimates derived from the analysis. However, the perturbation procedure does provide a definitive, affirmative answer to our second question. By allowing the fluid properties to vary with pressure and temperature the range of allowable temperature differences can be enlarged, at least for liquids. The actual factor by which this range can be increased is not well defined by the perturbation analysis for the reasons outlined above.

The results of the numerical solutions provided a second method for assessing the behaviour of the OB approximation. We initially believed that this approach would produce definitive answers to our problem and, in addition, clarify some of the quantitative uncertainties in the perturbation analysis. However, as will be shown subsequently, the interpretation and conclusions drawn from the numerical simulations are also plagued by the need for subjective judgements. In this case the main difficulty is determining when an approximate OB solution is sufficiently 'close' to the solution for the complete equation system.

From the results presented in section 5 it is observed that as the temperature difference across the cavity is increased (increasing Rayleigh number) both the strict and extended OB solutions show a smooth, progressive departure from the 'true' solution. Since there is no precipitous breakdown in the OB approximation a judgement must be made as to when (in terms of temperature difference) the strict and extended solutions are sufficiently different from the complete equation solution to be declared incorrect. Based on the simulation results presented here we have reached the conclusion that there is no unique answer to this question. Rather, the 'goodness' of the OB solutions depend on what quantities are of interest in the problem solution.

As shown in Figure 2 the overall heat transfer rate across the cavity is relatively insensitive to the OB approximation. Thus, if only overall, integrated energy transport is of interest then the OB equation systems may be used over very large temperature differences with only minor inaccuracies. Conversely, when the accurate prediction of a flow field is of concern then the OB approximation is seen to breakdown at much smaller imposed temperature differences. The actual point of this breakdown is subject to a judgement on the part of the analyst, though some reasonable quantitative estimates are possible. As an example, assume that errors in the velocity norm of up to $\sim 0{\cdot}0025$ are viewed as acceptable. In more physical terms, such an assumed error

bound corresponds to a maximum pointwise error in the velocity field of $\sim$ 10 per cent for both the strict and extended OB solutions. Referring to Figure 5 the specified tolerance on the velocity norm translates into acceptable maximum temperature differences of $\sim 11\,^{\circ}\mathrm{C}$ ($Ra = 45$) and $\sim 30\,^{\circ}\mathrm{C}$ ($Ra = 124$) for the strict and extended OB approximations, respectively. Comparing these limits to those produced by the perturbation analysis (Table III) shows that the perturbation results are slightly too conservative for the strict OB system and too optimistic for the extended OB equations.

Despite the inability to produce rigorous quantitative bounds on the use of the OB approximation, several specific statements and conclusions can be derived from the present study. In particular:

(i) The utility of a perturbation technique was demonstrated for the systematic analysis of various forms of the OB approximation.

(ii) The benefits of employing the extended OB approximation for liquid-saturated porous media were predicted via the perturbation analysis and verified by the numerical simulations.

(iii) The differences in the solutions to the OB equation systems and the complete equation system were illustrated and quantified as a function of Rayleigh number. Overall heat transfer quantities were judged to be insensitive to the type of equation system considered. The variations in the flow fields due to changes in equation system were noted and discussed.

(iv) Estimates of maximum allowable temperature difference were developed to bound the use of the OB approximations. For a water-saturated porous medium, temperature differences of approximately $10\,^{\circ}\mathrm{C}$ and $30\,^{\circ}\mathrm{C}$ were proposed for the strict and extended OB systems, respectively. These values were felt to provide solutions in reasonable agreement with solutions to the complete equation system.

(v) It is our opinion that the use of the OB approximation is a very convenient and powerful approach to analyzing natural convection problems, especially via numerical methods. However, the precise effects of the approximation on the solution are difficult to quantify, and thus great care must be taken when evaluating solutions to OB equations.

ACKNOWLEDGEMENTS

A preliminary version of this study was presented at the ASME-JSME Thermal Engineering Joint Conference in Honolulu, Hawaii, March 1983.

This work was performed at Sandia National Laboratories supported by the U.S. Department of Energy under contract DE-AC04-76DP00789.

APPENDIX: MATRIX AND FLUID PROPERTIES USED IN THE NUMERICAL SIMULATIONS

Matrix-glass (SiO_2)

$$\rho_s = 2650\,\mathrm{kg/m^3}$$

$$K_s = 1{\cdot}50\,\mathrm{J/ms\,^{\circ}C}$$

$$C_{ps} = 794\,\mathrm{J/kg\,^{\circ}C}$$

Water

$$\rho = \left(\sum_{n=0}^{5} a_n T^n\right) \Big/ (1 + a_6 T), \quad \text{kg/m}^3$$

$$\mu = b_0(10)^m, \quad m = b_1/(T - b_2), \quad \text{kg/ms} \tag{1}$$

$$K = \sum_{n=0}^{4} c_n T^n, \quad \text{J/ms °C}$$

$$C_p = 4180\ \text{J/kg °C} = \text{constant}$$

where the temperature T is in °C, and

$$a_0 = 999{\cdot}83952$$
$$a_1 = 16{\cdot}945176$$
$$a_2 = -7{\cdot}9870401 \times 10^{-3}$$
$$a_3 = -46{\cdot}170461 \times 10^{-6}$$
$$a_4 = 105{\cdot}56302 \times 10^{-9}$$
$$a_5 = -280{\cdot}54253 \times 10^{-12}$$
$$a_6 = 16{\cdot}879850 \times 10^{-3}$$
$$b_0 = 241{\cdot}4 \times 10^{-7}$$
$$b_1 = 247{\cdot}799$$
$$b_2 = 139{\cdot}998$$
$$c_0 = -0{\cdot}92247$$
$$c_1 = 1{\cdot}039538 \times 10^{-2}$$
$$c_2 = -2{\cdot}413453 \times 10^{-5}$$
$$c_3 = 2{\cdot}579836 \times 10^{-8}$$
$$c_4 = 1{\cdot}319252 \times 10^{-11}$$

REFERENCES

1. J. Boussinesq, *Theorie Analytique de la Chaleur*, Vol. 2, Gauthier-Villars, Paris, 1903.
2. A. Oberbeck, 'Uber die Warmeleitung der Flussigkeiten bei Berucksichtigung der Stromungen infloge von Temperature Differenzen', *Ann. Phys. Chem.*, **7**, 271–292 (1879).
3. D. D. Gray and A. Giorgini, 'The validity of the Boussinesq approximation for liquids and gases', *Int. J. Heat Mass Transfer*, **19**, 545–551 (1976).
4. R. K. MacGregor and A. F. Emery, 'Free convection through vertical plane layers—moderate and high Prandtl number fluids', *J. Heat Transfer*, **91**, 391–403 (1969).
5. A. Rubel and F. Landis, 'Laminar natural convection in a rectangular enclosure with moderately large temperature differences', *Proc. Fourth International Heat Transfer Conf.*, Paper NC 2.10, Paris-Versailles, 1970.
6. H. Shaukatullah and B. Gebhart, 'The effect of variable properties on laminar natural convection boundary-layer flow over a vertical isothermal surface in water', *Numerical Heat Transfer*, **2**, 215–232 (1979).
7. E. Leonardi and J. A. Reizes, 'Convective flows in closed cavities with variable fluid properties', in R. W. Lewis, K. Morgan and O. C. Zienkiewicz (eds), *Numerical Methods in Heat Transfer*, Wiley, Chichester 1981, pp. 387–412.
8. D. R. Kassoy and A. Zebib, 'Variable viscosity effects on the onset of convection in porous media', *Phys. Fluids*, **18**, 1649–1651 (1975).
9. J. M. Strauss and G. Schubert, 'Thermal convection of water in a porous medium: effects of temperature- and pressure-dependent thermodynamic and transport properties', *J. Geophysical Research*, **82**, 325–333 (1977).

10. R. J. Ribando and K. E. Torrance, 'Natural convection in a porous medium: effects of confinement, variable permeability and thermal boundary conditions', *J. Heat Transfer*, **95,** 42–48 (1976).
11. J. C. Ward, 'Turbulent flow in porous media', *J. Hydraul. Div., ASCE*, **19,** 1–12 (1969).
12. J. Bear, *Dynamics of Fluids in Porous Media*, American Elsevier Pub. Co., New York, 1972.
13. D. K. Gartling and C. E. Hickox, 'MARIAH—a finite element computer program for incompressible porous flow problems: theoretical background', *SAND79-1622*, Sandia National Laboratories, Albuquerque, NM, 1982.
14. D. K. Gartling and C. E. Hickox, 'MARIAH—a finite element computer program for incompressible porous flow problems: user's manual', *SAND79-1623*, Sandia National Laboratories, Albuquerque, NM, 1982.
15. C. E. Hickox and D. K. Gartling, 'A numerical study of natural convection in a horizontal porous layer subjected to an end-to-end temperature difference', *J. Heat Transfer*, **103**, 797–802 (1981).
16. C. E. Hickox and D. K. Gartling, 'A numerical study of natural convection in a vertical, annular, porous layer', *Int. J. Heat and Mass Transfer*, **28,** 720–723 (1985).
17. D. C. Reda, 'Natural convection experiments in a liquid-saturated porous medium bounded by vertical coaxial cylinders', *J. Heat Transfer*, **105,** 795–802 (1983).
18. D. C. Reda, 'Relaxation from forced downflow to buoyantly driven upflow about a vertical heat source in a liquid-saturated porous medium', *Proc. Fifth Engineering Mech. Div. Conf.*, ASCE, Laramie, Wyoming, 1984.
19. A. E. Gill, 'The boundary-layer regime for convection in a rectangular cavity', *J. Fluid Mech.*, **26,** 515–536 (1966).
20. K. H. Winters, 'The effect of conducting divisions on the natural convection of air in a rectangular cavity with heated side walls', *AIAA/ASME 3rd Joint Thermophysics, Fluids, Plasma and Heat Transfer Conf.*, Paper 82-HT-69, St. Louis, 1982.